ELASTIC-PLASTIC STRAIN OF A TITANIUM ALLOY UNDER PLANE STRESS STATE CONDITIONS

V. M. Zhigalkin, A. F. Nikitenko, and O. M. Usova

UDC 39.374

Elastic-plastic models are used in problems of the mechanics of mountain rocks when solving the question of the stress–strain state of a massif.

Results are presented in this paper of an experimental investigation whose aim was the confirmation of the suitability of a model of plastic strain of an anisotropically hardening medium [1, 2] for the simple and complex loading cases for fixed principal directions of the stress tensor, as well as the determination of the elastic-plastic properties of one of the titanium alloys for the biaxial stress state.

1. A sheet of titanium alloy 3V of 35-mm thickness is taken as initial material. Billets for the specimens were cut in the direction of the greatest dimension; this direction later agreed with the axial direction of the specimen. The transverse direction of the sheet agrees with the circumferential direction of the specimen.

The specimens to be tested had the following dimensions: outer diameter 30 mm, wall thickness in the working part 1 ± 0.01 mm. After fabrication the specimens were subjected to natural aging for 8 months.

Tests were performed on the testing machine UMÉ-10TM, which permitted loading the specimens with an axial force. The internal pressure in the specimen was produced by an additional manual continuous-action pump. The strains were measured by strain gauges with clock-type displays: axial by displays on a 50-mm base with 0.01-mm scale divisions, and circumferential by a micron display. The radial strain was determined by using a hypothesis about the elastic change in volume, while the radial stress was assumed zero.

A simultaneous change in the axial force and internal pressure for 5-7 sec was produced at each loading stage, the strain measurements were performed after a 5-min holding. The stability of the stress was assured by a continuous check on the operating mode of the testing machine.

The tests described below were carried out under biaxial tension, where $\sigma_z > \sigma_\varphi$ always. The loading trajectories were given on a plane with variables T, σ_2' ($\sigma_2' = T_{23} - T_{12}$) [2], where T, T_{12}, T_{23} are the principal tangential stresses related to the principal stress tensor components σ_1, σ_2, σ_3 by the known relationships $2T = \sigma_1 - \sigma_3$, $2T_{12} = \sigma_1 - \sigma_2$, $2T_{23} = \sigma_2 - \sigma_3$. The principal tangential stresses are related to the Lode parameter μ_σ characterizing the form of the stress state by the equality $\mu_\sigma = (T_{23} - T_{12})/T$. The parameter $\mu_{\Delta\sigma}$ characterizing the form of the loading [2] $\mu_{\Delta\sigma} = (\Delta T_{23} - \Delta T_{12})/\Delta T$ is introduced for the increment in the tangential stresses.

To describe the plastic behavior of the material, a model of an orthotropic medium is introduced [1, 2], whose basis is taking account of the anisotropy in the resistance to shears being developed together with the plastic strains on areas of the extremal values of the tangential stress. As tests show [3], the anisotropy of the plastic state depends on both the stress state achieved which is characterized by values of the maximal tangential stress T, the stress σ_2', and the loading direction.

Other illustrations of the anisotropy of the plastic state can be indicated by using tests when active loadings are realized in some principal directions of the stress tensor, while unloading is realized in others. The values of the kind of loading will here be $|\mu_{\Delta\sigma}| \geqslant 1$. Simple loadings are characterized by the growth of all extremal tangential stresses, values of the kind of loading $|\mu_{\Delta\sigma}| \leqslant 1$.

Novosibirsk. Translated from Zhurnal Prikladnoi Mekhaniki i Tekhnicheskoi Fiziki, No. 1, pp. 140-148, January-February, 1984. Original article submitted November 5, 1982.

 0021-8944/84/2501-0126$08.50

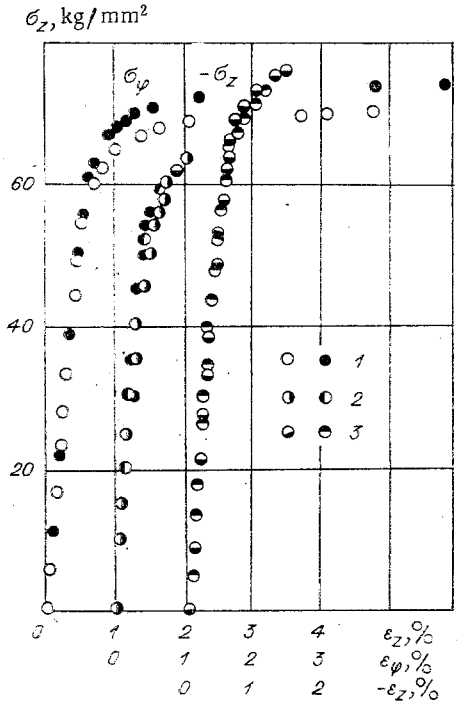

Fig. 1

The degree of anisotropy of the material was clarified by axial and circumferential tension tests on the specimens. The results of these tests are represented in Fig. 1 in the coordinate systems $\varepsilon_z - \sigma_z$ and $\varepsilon_\varphi - \sigma_\varphi$, where ε_z, ε_φ are the axial and circumferential strains, and σ_z, σ_φ are the normal axial and circumferential stresses. The following notation is introduced in Fig. 1: 1 is for axial tension; 2 is for circumferential tension; 3 is for axial compression. It is seen that the points of the circumferential tension curve were sufficiently close to points of the axial tension curves.

An analogous graph obtained during compression is shown in Fig. 1. It follows from an analysis of the axial tension and compression curves that they are not identical only on the hardening section. The difference in the provisional yield points, determined by a 0.2% tolerance in the residual strain, say, is approximately 11%.

Obtained from processing the curves represented in Fig. 1 is the elastic modulus $E = 1.14 \cdot 10^4$ kg/m^2, the Poisson ratio $\nu = 0.38$, the conditional yield point under tension $\sigma_{0.2} = 61.8$ kg/m^2, and under compression $\sigma_{0.2} = 68.9$ kg/mm^2. Let us turn to an analysis of the experimental data obtained for the plane stress state.

2. The loading trajectories in the experiments described below were single-linked (proportional loading) and double-linked (complex loading) broken lines.

Experimental results obtained under proportional loading conditions are represented in Fig. 2 in the $T_i - \Gamma_i$ coordinate system (T_i is the tangential stress intensity and Γ_i is the shear intensity) for the following values of the Lode parameter: $\mu_\sigma = \pm 1$; ± 0.75; ± 0.5; ± 0.25; 0. It is seen from Fig. 2 that in place of a single classical curve $T_i = T_i(\Gamma_i)$ there is a bundle of curves. The greatest deviation turns out to be between the tangential stress intensities for pure shear ($\mu_\sigma = 0$) and axial tension ($\mu_\sigma = -1$), and reaches 9%. As the plastic strains increase the bundle of curves is narrowed; the deviation between the corresponding tangential stress intensities does not exceed 6% (analogous ratios were indicated in [4, 6, 7]). Two series of tests were carried out under complex loading. In the first series the specimens were injected into the plastic state by axial tension ($\mu_\sigma = -1$) to the very same value of the axial stress $\sigma_z = 34$ kg/mm^2, then sections, lines, followed for loadings along which the value of the Lode parameter μ_σ changed while a constant value of the parameter $\mu_{\Delta\sigma}$ was retained. The parameter $\mu_{\Delta\sigma}$ took on the values $-1 \leqslant \mu_{\Delta\sigma} \leqslant \infty$.

In the second series of tests the specimens were injected into the plastic state by biaxial tension for $\mu_\sigma = 0$ up to the same value of axial stress as in the first series. The second sections of the loading trajectories are lines, for the loadings along which a constant value of $\mu_{\sigma v}$ equal to 0.5; 1; 3 was kept.

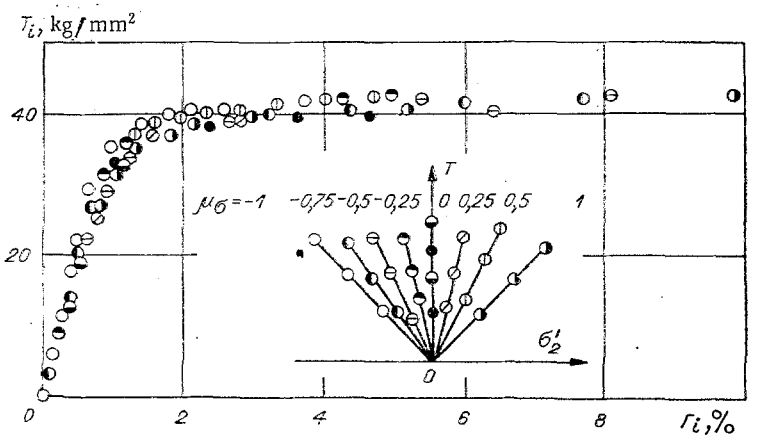

Fig. 2

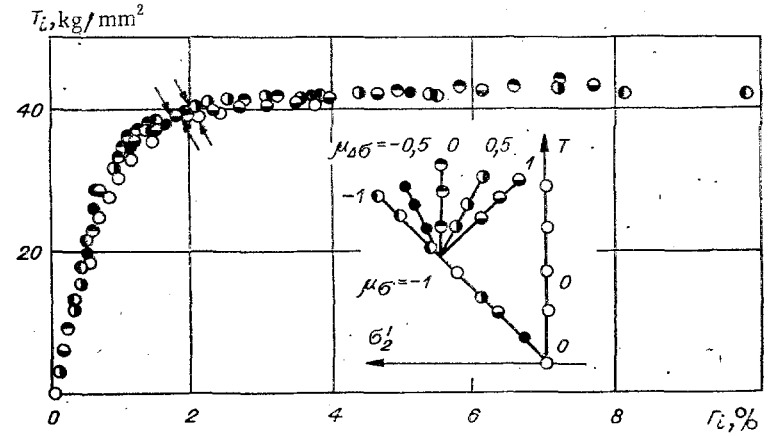

Fig. 3

Let us examine the test data for the first case. Here tests for simple loadings should be separated out, when the increments in the tangential stresses were positive at each step of the loadings, i.e., $\Delta T > 0$, $\Delta T_{12} > 0$, $\Delta T_{23} > 0$, $|\mu_{\Delta\sigma}| \leqslant 1$ and do not result in unloading on any of the systems of slip areas, and for loadings with unloading in the second systems of slip areas, i.e., $\Delta T \geqslant 0$, $\Delta T_{12} < 0$, $\Delta T_{23} > 0$, where $2 \leqslant \mu_{\Delta\sigma} \leqslant \infty$. These experimental results are, as before, represented in the T_i—Γ_i coordinate system in Fig. 3 (simple loading in the second sections of the loading trajectories) and in Fig. 4 (loading with unloading in the second slip area systems T_{12}). The beginning of the complex loading is shown by arrows. Superposed for comparison in Figs. 3 and 4 are points of the axial tension ($\mu_\sigma = -1$) and pure shear ($\mu_\sigma = 0$) curves.

As is seen from Fig. 3, for simple loadings the points of the curves $T_i = T_i(\Gamma_i)$ were arranged in the neighborhood of points of the axial tension curve. Points of the pure shear curve were below.

Points of the curves $T_i = T_i(\Gamma_i)$ are constructed in Fig. 4 for loading trajectories with unloadings in the slip areas T_{12}. These dependences also disclose a qualitative contradiction with the classical deduction of deformation theory that the nature of the loading path does not influence the dependence $T_i = T_i(\Gamma_i)$.

A more detailed arrangement of points of the relationship $T_i = T_i(\Gamma_i)$ in the second sections of the loading trajectories is represented in Fig. 5 as a function of the loading parameter $\mu_{\Delta\sigma}$. A regular deviation holds for points of the curves $T_i = T_i(\Gamma_i)$ under complex loading from points of the axial tension curve. Despite the growth of the tangential stress intensity for the loadings $\mu_{\Delta\sigma} = 2; 3$ and the growth of the shear intensity Γ_i, the points of the curves were arranged below the axial tension curve. For the loadings $\mu_{\Delta\sigma} \geqslant 4$ a "lune" is observed on the curves $T_i = T_i(\Gamma_i)$ in the neighborhood of the breakpoint of the loading trajectories, the shear intensities Γ_i grow with the diminution in the stress T_i on these sections. Under further loadings, the tangential stress intensities T_i again start to grow,

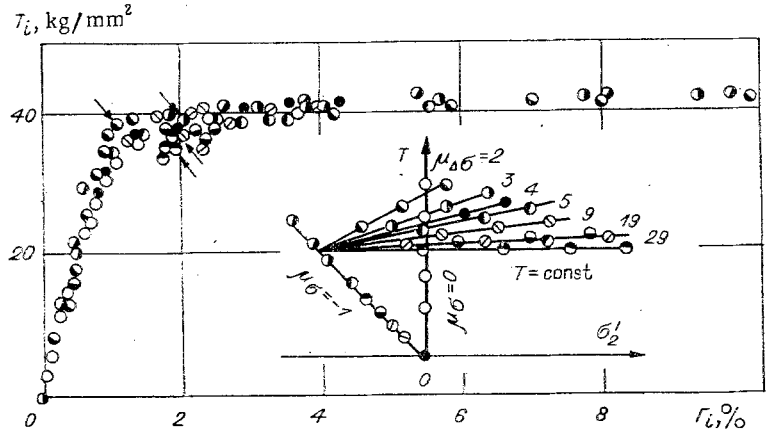

Fig. 4

points of the curves start to be "approached" and arranged in the neighborhood of the pure shear curve points.

According to the test data presented in Figs. 2-4, it can be noted:

1) Under proportional loadings the arrangement of the tangential stress intensity from the shear intensities depends on the kind of stress state; the curves corresponding to high absolute values of the Lode parameters μ_σ are located below;

2) under active loadings from the very same stress and strain states, the curves $T_i = T_i(\Gamma_i)$ are practically in agreement under complex loading conditions, and depend on the Lode parameter μ_σ at a time preceding the complex loading;

3) for loadings accompanied by a partial unloading in one of the principal plastic flow directions while active loadings continue in the other principal plastic flow directions, the location and shape of the curves $T_i = T_i(\Gamma_i)$ depend on the loading direction.

Within the framework of the phenomenological approach under consideration, the strain is represented as a sequence of shifts in the areas of the action of the principal tangential stresses T, T_{12}, T_{23}, called the T, T_{12}, T_{23} slip areas. It is convenient to represent the arbitrary loading $\Delta\sigma_1$, $\Delta\sigma_2$, $\Delta\sigma_3$ in the form [2]

$$\begin{vmatrix} \Delta\sigma_1 & 0 & 0 \\ 0 & \Delta\sigma_2 & 0 \\ 0 & 0 & \Delta\sigma_3 \end{vmatrix} = \Delta\sigma_n \begin{vmatrix} 1 & 0 & 0 \\ 0 & 1 & 0 \\ 0 & 0 & 1 \end{vmatrix} + \Delta T \begin{vmatrix} 1 & 0 & 0 \\ 0 & 0 & 0 \\ 0 & 0 & -1 \end{vmatrix} + \Delta\sigma_2' \begin{vmatrix} 0 & 0 & 0 \\ 0 & 1 & 0 \\ 0 & 0 & 0 \end{vmatrix}, \tag{2.1}$$

where $2\Delta\sigma_n = \Delta\sigma_1 + \Delta\sigma_3$; $\Delta\sigma_2' = \Delta T_{23} - \Delta T_{12} = \mu_{\Delta\sigma}\Delta T$.

The second and third tensors in the right side of the partition (2.1) acquire a special meaning associated with the action of the principal tangential stresses. The first tensor describes the change in volume and does not influence the plastic strain.

Let the action of the third tensor be such that the stress increment $\Delta\sigma_2'$ causes an elastic strain increment

$$\Delta\varepsilon_2' = \Delta\varepsilon_2 - \frac{1}{2}(\Delta\varepsilon_1 + \Delta\varepsilon_3) = \frac{1}{2}(\Delta\Gamma_{23} - \Delta\Gamma_{12}),$$

where $\Delta\varepsilon_1$, $\Delta\varepsilon_2$, $\Delta\varepsilon_3$ are increments of the principal strains ε_1, ε_2, ε_3 ($\varepsilon_1 \geqslant \varepsilon_2 \geqslant \varepsilon_3$); $\Delta\Gamma = \Delta\varepsilon_1 - \Delta\varepsilon_3$, $\Delta\Gamma_{12} = \Delta\varepsilon_1 - \Delta\varepsilon_2$, $\Delta\Gamma_{23} = \Delta\varepsilon_2 - \Delta\varepsilon_3$ are the increments of the principal shears on the slip areas.

In this case the plastic strain increments are caused by the action of the maximal tangential stress T. Then a rectangular parallelepiped cut out of the body by the principal shear areas will actually be weakened only on the side surfaces. But the element along the axis parallel to the side surfaces will be strained elastically. This is a state of incomplete plasticity.

Under further loadings, slips on other slip areas can appear and be developed in addition to the slips at the principal shear areas. The element is deformed into a state of full

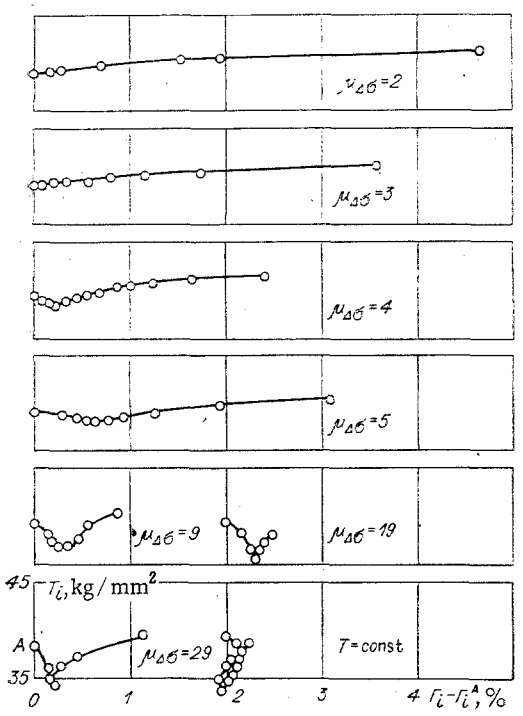

Fig. 5

plasticity. In this case the material is shattered into blocks by two systems of slip areas. Among these blocks it is possible to extract a preferred number having a shape close to irregular octahedra with a face direction close to the slip area direction [1].

Using this scheme for material element deformation, cited in [1, 2], it is possible to recognize over what areas shears represented in Figs. 6 and 7 in the tangential stress T_{ij}—shear Γ_{ij} ($i < j$; $i, j = 1, 2, 3$) coordinates, are realized on the slip areas. The dependence of the stress $\sigma_2' = T_{23} - T_{12}$ on the strain $\varepsilon_2' = (\Gamma_{23} - \Gamma_{12})/2$ is represented there. In the first sections of the loading trajectories the specimens are injected into a state of full plasticity with slip areas T, T_{12} by axial tension, and the stress is zero on the areas T_{23}. In the second sections of the loading trajectories, unloading is realized for the finish loadings $\mu_{\Delta\sigma} = 5$ (Fig. 6), $\mu_{\Delta\sigma} = 19$ (Fig. 7) in one of the two principal directions of plastic flow T_{12}, partial hardening sets in here in the unloading direction, as does passage to a state analogous to incomplete plasticity [1].

The nature of the change in the dependences $T_{ij}(\Gamma_{ij})$ in the complex loading section is the following. An abrupt increase in the tangential modulus as compared to the tangential modulus at a time preceding the breakpoint in the loading trajectory and the beginning of

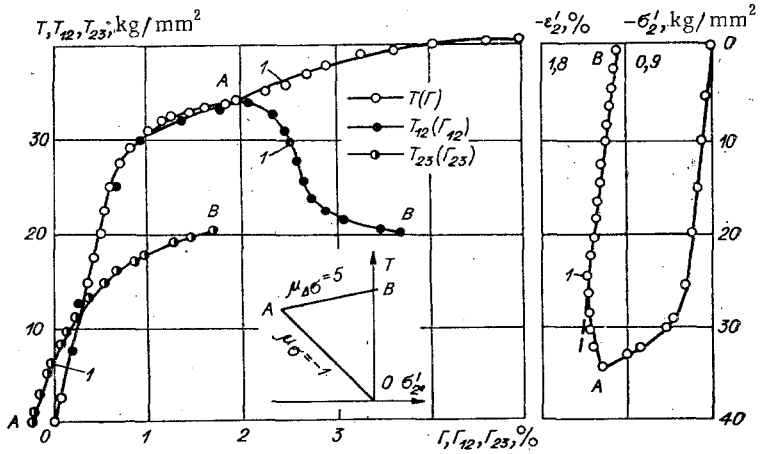

Fig. 6

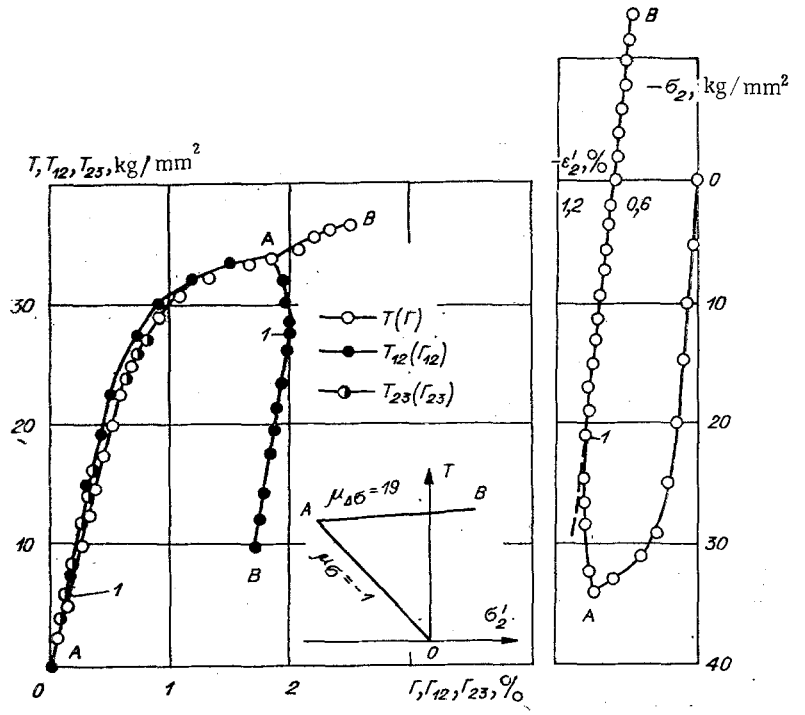

Fig. 7

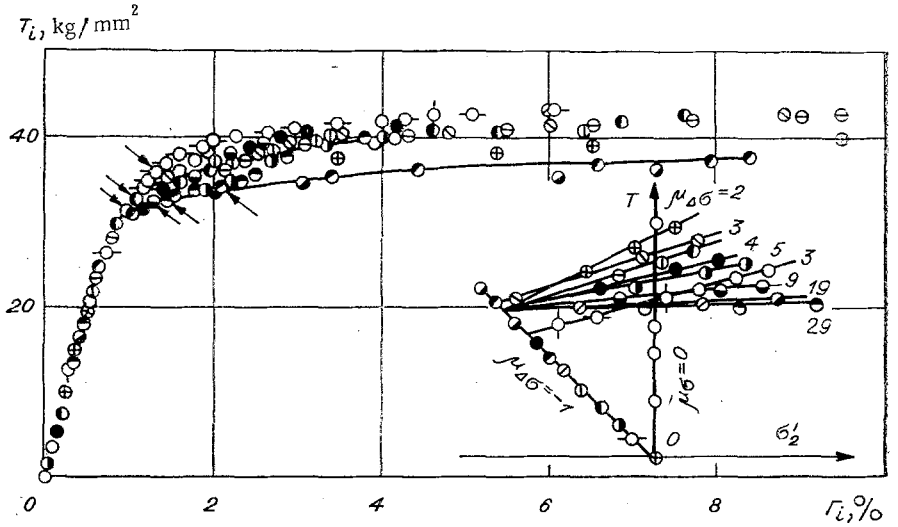

Fig. 8

the complex loading occurs at the point A of the curve T = T(Γ). The nature of the change in the modulus is retained under subsequent finish loadings.

For loadings $\mu_{\Delta\sigma}$ = 5 (see Fig. 6), unloading is realized on the areas T_{12}, but as the tangential stress T_{12} diminishes, the shear Γ_{12} continues to grow. As the stress T_{23} grows on the areas T_{23}, the shears Γ_{23} grow less than the elastic modulus with the tangential modulus.

For loadings $\mu_{\Delta\sigma}$ = 19 (see Fig. 7), initially the shears grow with the diminution in the stress T_{12} at the beginning of the complex loading. Under subsequent loadings, starting with the point 1, the dependence $T_{12} = T_{12}(\Gamma_{12})$ becomes linear with a tangential modulus greater than the elastic modulus. The dependence $T_{23} = T_{23}(\Gamma_{23})$ is also linear, with a modulus equal to the elastic, and for $T_{23} \geqslant 20$ kg/mm^2 the modulus becomes less than the elastic.

The action of the stress σ_2' in the second sections of the loading trajectory is such that it causes only elastic strains ε_2'. As is seen from Figs. 6 and 7, starting from the point 1 the dependence $\sigma_2' = \sigma_2'(\varepsilon_2')$ becomes linear. Points of the dependence are on a line whose slope

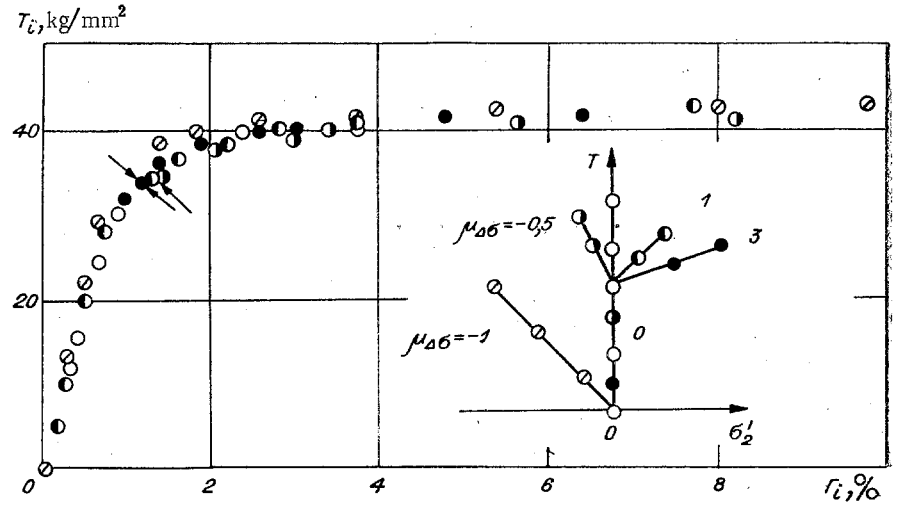

Fig. 9

agrees with the elastic slope; it is shown by dashed lines in the figures. The linear nature of the dependence is retained up to fracture.

An analogous restoration of the elastic relation was observed in the second principal direction for all specimens at loadings $\mu_{\Delta\sigma} \geqslant 3$.

Therefore, for loadings $\mu_{\Delta\sigma} \geqslant 1$ from the state of full plasticity with unloading in one of the principal directions of plastic flow T_{12}, plastic shears occur on slip areas T; unloading with hardening is realized on the areas T_{12}. This hardening makes the dependence of the maximal tangential stress on the shear different from the "single curve" $T = T(\Gamma)$ also, independently of the form of the stress state.

Points of the curves $T = T(\Gamma)$ are represented in Fig. 8 for loadings $\mu_{\Delta\sigma} \geqslant 1$ from the state of full plasticity. The nature of the change in the dependence $T = T(\Gamma)$ is analogous to the nature of the dependence $T = T(\Gamma)$ in Figs. 6 and 7. Superposed here for comparison are points of the axial tension and pure shear curves. Arrows indicate the beginning of the complex loading. The maximal deviation of points of the curve along the ordinate is 25%. Because of the abrupt increase in the tangential modulus of the curve $T = T(\Gamma)$ at the beginning of the complex loading, these dependences were above the curve $T = T(\Gamma)$ for axial tension. The last point on each curve corresponds to the time of specimen fracture. It is seen from Fig. 8 that the strength for specimens tested in the complex loading program with $\mu_{\Delta\sigma} \geqslant 3$ rose on the average to 43 kg/mm² while it is 36 kg/mm² under axial tension.

Let us examine the test data of the second series of tests. The specimens were injected into the plastic state by pure shear (the state of incomplete plasticity), plastic shears occurred on areas of the action of the maximal tangential stress T. Both active finish loading (the finish loading parameter took the values $\mu_{\Delta\sigma} = -0.5$; 1; 0) and unloading on the areas T_{12} ($\mu_{\Delta\sigma} = 3$) were realized under complex loadings.

Presented in Fig. 9 are dependences of the tangential stress intensity T_i on the shear intensity Γ_i for these tests. Superposed here for comparison are points of the axial tension and pure shear curves. The points of the curves were in the neighborhood of points of the pure shear curve. The test data indicate the appearance and development of plastic shears on the slip areas T_{12} ($\mu_{\Delta\sigma} = -0.5$) or T_{23} ($\mu_{\Delta\sigma} = 1$; 3) in addition to the plastic shears in the principal slip areas T. Partial hardening does not occur in the unloading direction T_{12} if there are no plastic shears in these areas. Relative displacement of the strong elements, which is a consequence of active finish loading in the directions T and T_{23}, continues in the unloading direction.

The tests examined permit making a deduction about the suitability of the plastic deformation scheme proposed in [1, 2] for the simple and complex loading cases when plastic deformation occurs in some principal directions and unloading in others. Plastic deformations are due mainly to shears in planes close to the planes of action of the principal tangential stresses.

There are directions in the material and forms of finish loading from the stress state achieved for which elastic deformation occurs in these directions in addition to the plastic

deformation in others. For deformation of the alloy 3V from the state of full plasticity with finish loadings $\mu_{\Delta\sigma} \geqslant 3$, an elastic relationship in the second principal (circumferential) direction is restored. Restoration of the elastic relationship results in a 20% rise in the strength of the material.

LITERATURE CITED

1. S. A. Khristianovich, "Deformation of a hardening plastic material," Izv. Akad. Nauk SSSR, Mekh. Tverd. Tela, No. 2 (1974).
2. E. I. Shemyakin, "Anisotropy of the plastic state," ChMMSS, No. 4 (1973).
3. V. M. Zhigalkin, "On the nature of plastic material strengthening. Report II," Probl. Prochn., No. 2 (1980).
4. O. A. Shishmarev, "Experimental investigation of the similarity of stress and strain deviators in steel specimens," Izv. Vyssh. Uchebn. Zaved., Mashinostroenie, No. 1 (1971).
5. G. L. Lindin, "On the strengthening of an elastic-plastic body," Zh. Prikl. Mekh. Tekh. Fiz., No. 3 (1976).
6. O. A. Shishmarev, "Influence of the kind of stress deviator on the plastic deformation of steels," Inzh. Zh. Mekh. Tverd. Tela, No. 5 (1966).
7. O. A. Shishmarev, "Calculation of plastic deformation according to flow theories with the influence of the kind of stress deviator taken into account," Vestn. Akad. Nauk BSSR, Ser. Fiz.-Mat. Nauk, No. 4 (1979).

MICROSTRUCTURES OF PULSE-HEATED TITANIUM ALLOYS

A. É. Verte and B. A. Goshmer

UDC 536.33+539.319

A metal shows an increase in dislocation density near the point of action of a laser beam or a high-density electron beam. However, such studies have not been performed with heating by thermal radiation.

Here we report on the microstructures for OT4-0 and OT4-1 titanium alloys heated by thermal radiation. Increased dislocation densities are found in the surface layers, and slip lines occur in the grains.

The experiments were performed with specimens made from rolled sheets of thickness ($1-1.5\cdot10^{-3}$ m), which were heated to 1070°K by a thermal radiation flux of density $2.5\cdot10^5$ W/m^2 in an apparatus in which the radiation was provided by halogen lamps and the rise time to the maximum value was 0.5 sec. A specimen was a strip of width $3\cdot10^{-2}$ m cut from the irradiated sheet, with the end processed as a polished section prepared by mechanical polishing with abrasives, diamond paste, and electrochemical polishing. The section should be of good quality without erosion of the lateral edges, which contain most of the information on the microstructure, and there should be no signs of etching at a magnification of 600 in order to provide reproducible results in examining the dislocation structure. These requirements are met by polishing in an electrolyte of the following composition: 60% H_2SO_4,

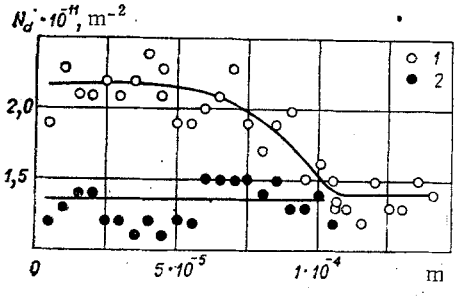

Fig. 1

Novosibirsk. Translated from Zhurnal Prikladnoi Mekhaniki i Tekhnicheskoi Fiziki, No. 1, pp. 148-150, January-February, 1984. Original article submitted December 2, 1982.

0021-8944/84/2501-0133$08.50